

# Encoding of Visual Information by LGN Bursts

PAMELA REINAGEL,<sup>1</sup> DWAYNE GODWIN,<sup>2</sup> S. MURRAY SHERMAN,<sup>2</sup> AND CHRISTOF KOCH<sup>3</sup>

<sup>1</sup>*Sloan Center for Theoretical Neuroscience, California Institute of Technology, Pasadena, California 91125;* <sup>2</sup>*Department of Neurobiology, State University of New York at Stony Brook, Stony Brook, New York 11794;* and <sup>3</sup>*Computation and Neural Systems Program, California Institute of Technology 139-74, Pasadena, California 91125*

**Reinagel, Pamela, Dwayne Godwin, S. Murray Sherman, and Christof Koch.** Encoding of visual information by LGN bursts. *J. Neurophysiol.* 81: 2558–2569, 1999. Thalamic relay cells respond to visual stimuli either in burst mode, as a result of activation of a low-threshold  $\text{Ca}^{2+}$  conductance, or in tonic mode, when this conductance is inactive. We investigated the role of these two response modes for the encoding of the time course of dynamic visual stimuli, based on extracellular recordings of 35 relay cells from the lateral geniculate nucleus of anesthetized cats. We presented a spatially optimized visual stimulus whose contrast fluctuated randomly in time with frequencies of up to 32 Hz. We estimated the visual information in the neural responses using a linear stimulus reconstruction method. Both burst and tonic spikes carried information about stimulus contrast, exceeding one bit per action potential for the highest variance stimuli. The “meaning” of an action potential, i.e., the optimal estimate of the stimulus at times preceding a spike, was similar for burst and tonic spikes. In within-trial comparisons, tonic spikes carried about twice as much information per action potential as bursts, but bursts as unitary events encoded about three times more information per event than tonic spikes. The coding efficiency of a neuron for a particular stimulus is defined as the fraction of the neural coding capacity that carries stimulus information. Based on a lower bound estimate of coding efficiency, bursts had ~1.5-fold higher efficiency than tonic spikes, or 3-fold if bursts were considered unitary events. Our main conclusion is that both bursts and tonic spikes encode stimulus information efficiently, which rules out the hypothesis that bursts are nonvisual responses.

## INTRODUCTION

The dorsal lateral geniculate nucleus of the thalamus (LGN) is the primary relay by which visual information from the retina reaches the cortex. Retinal ganglion cells are connected to LGN relay cells with relatively little divergence or convergence, so the spatial receptive-field organization that the LGN inherits from the retina is largely preserved. Rather than extracting new spatial features in the visual input, the function of the LGN may be to selectively transmit or “gate” visual information as a function of time. Transmission could be facilitated, inhibited, or filtered by the many nonretinal inputs to the LGN relay cell, for example, from the brain stem, thalamic reticular nucleus, or cortex (reviewed in Sherman and Guillery 1996; Sherman and Koch 1986; Singer 1977; see also Crick 1984).

One mechanism by which the thalamus might gate visual information is through controlled activation of  $I_t$ . The inward current  $I_t$  is attributed to a low-threshold calcium conductance (Guido and Lu 1995; McCormick 1992; McCormick and

Feeseer 1990; Steriade and Llinás 1988), which is voltage dependent (Coulter et al. 1989). When this conductance is inactive, at relatively depolarized membrane potentials, a brief depolarizing pulse (such as might be generated by a presynaptic retinal action potential) will cause an LGN relay cell to fire one or a few unitary action potentials. If the cell experiences a prolonged hyperpolarization ( $\geq 100$  ms),  $I_t$  becomes primed or “deinactivated” (Jahnsen and Llinás 1984a,b). Once this has occurred, the cell will respond to a depolarizing pulse with a characteristic burst of action potentials riding the crest of a slower calcium spike (Scharfman et al. 1990).

Thus each individual cell can be described as having a response mode (burst or tonic) at each point in time, depending on the instantaneous degree of  $I_t$  inactivation. To a first approximation, the mode can be regarded as binary (Coulter et al. 1989). When a cell is in tonic mode, it is poised to fire one or more individual action potentials in response to an input, if it fires at all; when a cell is in burst mode, its next response will be a stereotyped burst. The bursts associated with  $I_t$  can be distinguished reliably from tonic spikes on the basis of its interspike interval (ISI) pattern (Lu et al. 1992). Therefore, on the basis of extracellular recordings, one can infer the underlying response mode of a cell at the time of each observed response.

Under some conditions, such as low arousal or sleep, LGN cells become uncoupled from retinal input (Coenen and Vendrik 1972; Fourment et al. 1984; Livingstone and Hubel 1981). In this physiological state the LGN relay cells are relatively hyperpolarized, such that  $I_t$  is in a primed state much of the time, i.e., the cells are predominantly in burst mode. LGN cells then burst rhythmically and synchronously, due to the biophysical properties of the current in conjunction with other intrinsic membrane properties and local circuit properties (Bal and McCormick 1997; McCormick and Feeseer 1990; Steriade and Llinás 1988; von Krosigk et al. 1993). These observations suggest the hypothesis that whenever an LGN cell enters burst mode, the cell becomes uncoupled from visual input. This hypothesis predicts that when bursts occur during visual stimulation, individual bursts will not be related systematically to stimulus events.

In lightly anesthetized or awake animals, a mixture of tonic spikes and arrhythmic bursts is found, with the ratio of responses occurring in the two modes falling on a continuum (Guido et al. 1992, 1995; Guido and Weyand 1995; Mukherjee and Kaplan 1995). Under these conditions, when bursting was varied pharmacologically, bursts were found to correlate with enhanced detectability of near-threshold visual stimuli. The improvement, due in part to the reduction in spontaneous

The costs of publication of this article were defrayed in part by the payment of page charges. The article must therefore be hereby marked “advertisement” in accordance with 18 U.S.C. Section 1734 solely to indicate this fact.

activity, was at the expense of response linearity that may be important for stimulus discrimination (Godwin et al. 1996b; Guido et al. 1995). The correlation between detectability and burst fraction suggests the hypothesis that the bursts directly encode visual information. This hypothesis predicts that individual bursts can be systematically related to individual stimulus events.

In the present study, we set out to determine whether these differences between burst and tonic firing response modes correspond to differences in visual information transmission properties. The “information” in a neural response is defined as the extent to which observing the response would reduce a receiver’s uncertainty about the particular visual stimulus, compared with not observing the response and relying only on the average statistics of that stimulus (Rieke et al. 1997; Shannon and Weaver 1963). We estimated the information using a stimulus reconstruction method (Bialek et al. 1991; Rieke et al. 1997). We found that both burst and tonic firing modes relay roughly equivalent amounts of stimulus-related information to visual cortex. Preliminary results of this study have been reported in abstract form (Reinagel et al. 1997).

## METHODS

### *Physiological methods*

**PREPARATION.** We performed experiments on cats that we initially anesthetized with 3.5% halothane and then maintained after surgery on 0.5–1.5% halothane in a 70/30 mixture of N<sub>2</sub>O/O<sub>2</sub>. Cats were paralyzed with gallamine triethiodide (5.0 mg) and were artificially respired through a tracheal cannula. Paralysis was maintained with gallamine triethiodide (3.6 mg/h) and tubocurarine (0.7 mg/h). We treated wound margins and pressure points with a topical anesthetic. Cats were placed in a stereotaxic apparatus for recordings. Rectal temperature, heart rate, and end-tidal CO<sub>2</sub> were continuously monitored and maintained within normal physiological limits.

Access to the LGN was obtained through a craniotomy (5.0 mm diam) centered at A 5.0, L 9.0. We recorded from single neurons in the LGN A-laminae with a tungsten-in-glass recording electrode [impedances 8–14 M $\Omega$  (Godwin 1993)]. Neuronal activity was amplified, displayed on an oscilloscope, voltage window discriminated, and stored on computer as spike arrival times with a resolution of 0.1 ms. A pair of insulated tungsten electrodes (500- $\mu$ m exposed tips) were lowered to rest on either side of the optic chiasm, through a second craniotomy centered at A 13.0, L 0.0. To measure conduction velocity, we orthodromically activated LGN neurons through these electrodes using 0.1-ms, 100- to 500- $\mu$ A square-wave pulses at a frequency of 1 Hz.

After dilating the pupils with atropine sulfate, we protected the corneas with contact lenses selected to provide a focused image to the retina of stimuli presented on a tangent screen positioned 57.0 cm in front of the nodal points of the eyes. We used a fiber optic light source to plot retinal landmarks (including the optic disk, area centralis, and major retinal blood vessels) on the tangent screen by tapetal reflection (Pettigrew et al. 1979).

In a subset of experiments, we recorded and delivered drugs with a tungsten-in-glass recording electrode (impedances 8–14 M $\Omega$ ) combined with a multibarreled drug pipette (Godwin 1993). We applied *trans*-(1S,3R)-1-amino-1,3-cyclopentanedicarboxylic acid (ACPD, 30 mM), a selective agonist to metabotropic glutamate receptors, to depolarize the membrane potential of LGN cells and to switch the response state from burst to tonic (Godwin et al. 1996b). The amount of ACPD applied is expected to depolarize the cell by  $\sim$ 10 mV (McCormick and von Krosigk 1992). Conventional iontophoretic controls were performed to preclude nonspecific effects of pH and

current. The response of the cell was determined before, during, and after application of the drug.

**CLASSIFICATION OF CELLS.** We initially determined neuronal receptive-field position, center sign, size, and ocularity by plotting neuronal activity in response to small spots of light projected onto the tangent screen. We then replaced the tangent screen with a Tektronix 608 oscilloscope monitor for the presentation of test stimuli. We classified all neurons as X or Y using a battery of tests, including latency to electrical stimulation from optic chiasm, linearity of spatial summation, center size, and the response of the surround to a large, rapidly moving stimulus of opposite sign to the receptive-field center.

**VISUAL STIMULATION.** We presented a time-varying contrast signal to the cells on a Tektronix 608 monitor, with a space average luminance  $L_0 = 60$  cd/m<sup>2</sup>. Monitor contrast was controlled by a computer via a 12-bit A/D converter using the Picasso stimulus generation system (Innisfree).

The spatial form of the stimulus was a stationary sinusoidal grating presented through a fixed circular aperture (Fig. 1A). This particular spatial structure is not relevant to the analysis except that LGN relay cells respond well to its temporal modulation. We define contrast as  $(L_{\max} - L_{\min}) / (L_{\max} + L_{\min})$ , where  $L_{\max}$  and  $L_{\min}$  refer to the maximum and minimum luminance of the grating.

The contrast of the grating was randomly varied as a function of time (Fig. 1B) according to a Gaussian amplitude distribution (Fig. 1C) with a flat spectrum up to a cutoff frequency (CF; Fig. 1D). The random sequences were generated by selecting pseudorandom values in the frequency domain, imposing the frequency cutoff, and inverse Fourier transforming the result (Press et al. 1992; F. Gabbiani, personal communication). Each stimulus was derived from a unique seed to the pseudorandom number generator; no specific random sequence was ever repeated. Each contrast value was presented for the duration of one 4.96-ms “frame” before jumping to the next contrast value. A single “trial” refers to continuing such contrast modulation with fixed statistics for a total trial time of 4 (or occasionally 20) minutes. One 4-min trial generally constitutes enough data for a comparison of burst to tonic spikes, as described in *Numerical methods*.

Phase reversal of the grating was not permitted, so that the intensity in the receptive-field center was always less than or equal to background for OFF cells and always greater than or equal to background for ON cells. Therefore higher “contrast” always corresponds to a more excitatory stimulus for the cell. When displaying the Gaussian distribution, all negative values were displayed as zero contrast, and values greater than one were displayed as a contrast of one. We report only results obtained using stimuli whose mean contrast  $\mu$  was at least  $2\sigma$  above zero and  $2\sigma$  below one. Therefore, at most, 2% of the stimulus values were adjusted in this way, which resulted in a reduction in the entropy of the stimulus of at worst 2%, compared with the originally generated Gaussian distribution.

In different trials, the standard deviation ( $\sigma$ ) of the contrast was varied from 0.001 to 0.2, the temporal cutoff (CF) was varied from 1 to 32 Hz, and the mean contrast ( $\mu$ ) was varied between 0.2 and 0.5. Preliminary experiments revealed that the amplitude of the contrast modulations ( $\sigma$ ) had the strongest effects on firing rate and coding properties, and therefore was explored in detail (see RESULTS). In most experiments,  $\mu$  was held constant at the estimated midpoint of the cell’s contrast sensitivity range (typically 0.3–0.4), and CF was between 8 and 32 Hz.

Because the stimulus could theoretically assume  $2^{12}$  distinct values and was updated every 4.96 ms, the maximum possible stimulus entropy rate was  $2.4 \times 10^3$  bits/s. The actual stimulus entropy was substantially less than this, mainly because of the temporal correlations imposed by the cutoff frequency (CF). An 8-Hz cutoff would reduce the entropy to  $\sim$ 96 bits/s, for example. The distribution of contrast values had a less marked effect on the entropy. For example, an approximate Gaussian with  $\mu = 0.5$  and  $\sigma = 0.1$  had an effective entropy only 10% lower than that of a uniform distribution of values.

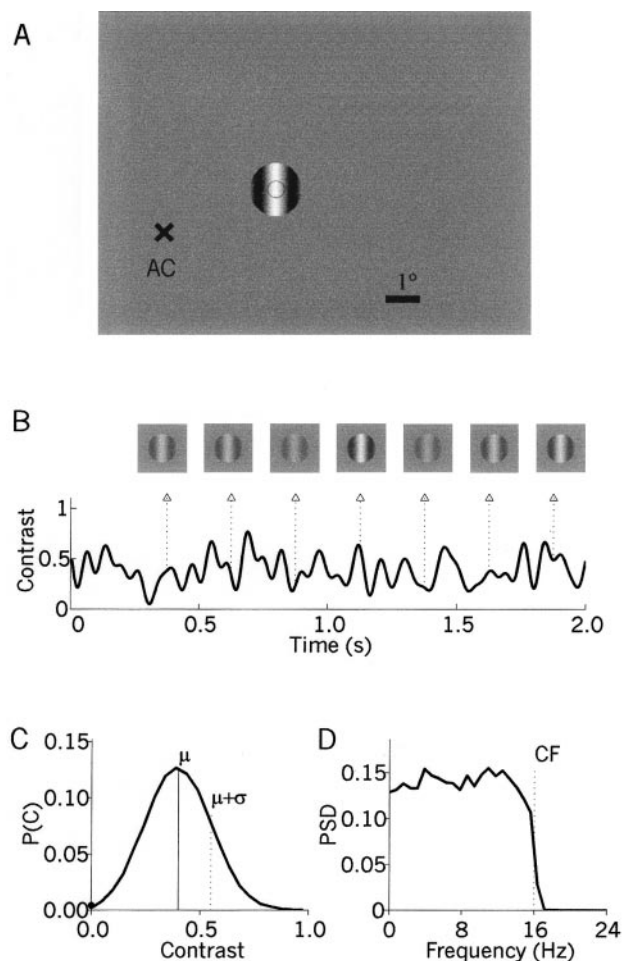


FIG. 1. Schematic diagram of the spatial structure of the stimulus. *A*: the entire oscilloscope screen is represented by the gray rectangle (scale bar  $1^\circ$  visual angle). This stimulus is for an ON cell with a receptive field center diameter of  $0.5^\circ$  (black circle), located at an eccentricity of  $3.3^\circ$  relative to the area centralis (X). The spatial period of the grating was set to twice the diameter of the receptive field center. An excitatory phase of the grating was centered on the center of the cell's receptive field, with the opposite phase positioned within the surround. The aperture was centered on the receptive field center and its diameter adjusted to 1.5 periods, to encompass the inhibitory flank. The background was set to the mean luminance:  $(L_{\max} + L_{\min})/2$ . The spatial structure was optimized for each cell and then held constant for all trials on that cell. *B*: contrast of the static grating as a function of time. We express contrast of the grating according to the convention  $(L_{\max} - L_{\min}) / (L_{\max} + L_{\min})$ . Contrast was updated to a new randomly chosen value every 4.96 ms. Stimulus time course is shown for the 1st 2 s of a 4-min trial. At the indicated time points, the appearance of the stimulus in the vicinity of the receptive field is shown above. *C*: The actual distribution of contrast values over the entire 4-min trial is shown as the probability  $P(C)$  for each contrast range ( $n = 49,152$  frames, bins of width 5% contrast contain  $\sim 100$  discrete contrast values each). For this stimulus, the random contrast values were chosen from a Gaussian distribution with a mean ( $\mu$ ) of 0.4 and a standard deviation ( $\sigma$ ) of 0.15. The closed circle indicates the number of negative values in the originally generated distribution, which were displayed as zero contrast (i.e., the illumination within the aperture was uniform and equal to the background illumination). *D*: actual distribution of temporal frequencies is shown by the power spectral density (PSD) of the stimulus, in units of  $\text{Hz}^{-1}$ . In this trial the random contrast values were chosen from a temporal frequency distribution that was flat (white spectrum) up to a cutoff frequency (CF) of 16 Hz.

The resulting stimulus entropy rates typically exceeded the coding capacity of the cells (see *Numerical methods*), such that the stimuli challenged the cells' capacity for information.

## Numerical methods

All calculations were carried out in Matlab 5.0 (MathWorks).

**BURST IDENTIFICATION.** We classified burst responses from extracellularly recorded spike arrival times using previously published criteria (Godwin et al. 1996b; Guido et al. 1995; Lu et al. 1992). Our operational definition of a "burst" is a group of action potentials each of which is  $<4$  ms apart, with the first spike in a burst preceded by a period of  $>100$  ms devoid of spiking activity. Previous intracellular recordings in this preparation (Lu et al. 1992) demonstrated that this ISI pattern is a stringent criterion for identifying the bursts that are associated with the low-threshold calcium conductance that results from  $I_t$ . As additional evidence that these burst events in our data reflected  $I_t$  activity, in a subset of experiments we also showed that these events were sensitive to application of the metabotropic agonist ACPD (data not shown), which slightly depolarizes LGN relay cells and thereby inactivates  $I_t$  (Godwin et al. 1996b).

Burst identification was based on the spike times as recorded, at 0.1-ms resolution. For subsequent calculations of coding capacity and stimulus reconstruction, the times of spikes were binned at the same resolution as the stimulus update rate, 4.96 ms. The value in each time bin was equal to the number of spikes that occurred in that interval. Thus when all the spikes of a burst were analyzed, information about the number of spikes in each burst was preserved. When we analyzed the bursts as unitary events (Bair et al. 1994), we discarded information about the number of spikes in each burst and replaced each burst with a single event defined to occur at the time of the first action potential of the burst.

**ESTIMATION OF SPIKE TRAIN CODING CAPACITY.** Given an observed set of neural responses to a specific set of stimuli, the information the responses could convey about the stimuli is limited by the total variability of the response, i.e., the diversity of different spike trains the cell uses across the entire range of stimuli. In our analysis we represented neural responses, or components of these responses (tonic or burst), as "spike trains," in which the value in each time bin reflects the number of action potentials in that interval. The variability of these spike trains may be quantified in an information theoretical framework by an entropy rate, which has units of bits per second. The entropy rate of a spike train is analogous to the "baud rate" of a computer modem: a spike train from an ensemble with a higher entropy rate has greater capacity for carrying encoded information, although this capacity may or may not be fully utilized. We call this entropy rate the "coding capacity" of the response. Note that this is different from the "channel capacity" of the neuron (Shannon and Weaver 1963), which is the maximum coding capacity the cell could have to any set of stimuli, using any code, based only on its physical limitations.

The maximal entropy rate for any spike train with firing rate  $r$  (in Hz) binned at resolution  $\Delta t$  (in seconds) can be approximated as

$$H_{\max} = r \log_2 \left( \frac{e}{r \Delta t} \right) \text{ bits/s} \quad (1)$$

where  $e$  is the base of the natural logarithm (MacKay and McCulloch 1952). This approximation is accurate in the limit that  $r \Delta t \ll 1$ . For the bin size we used ( $\Delta t = 4.96$  ms) and the range of firing rates observed, this function is increasing with the rate  $r$  ( $H_{\max}$  decreases with  $r$  only at firing rates exceeding  $r = 200$  Hz).

The observed interval distribution of our spike trains can be used to place a more accurate upper limit on their entropy. If the statistics of the spike train are completely characterized by its mean firing rate  $r$  and interspike interval distribution  $P(\tau)$  (in other words, if the spike train is a renewal process), then the entropy rate of the spike train is given by

$$H_{\text{capacity}} = -r \sum P(\tau) \log_2 P(\tau) \text{ bits/s} \quad (2)$$

where the sum is taken over all observed interspike intervals, and  $r$  is the number of intervals per second (i.e., the firing rate) (Rieke et al. 1993; Warland et al. 1997; Zador 1998). Note that in the limit of a perfectly regular spike train,  $P(\tau) = 1$  for one interspike interval length  $\tau$  and  $P(\tau) = 0$  for all the other interval lengths, resulting in a coding capacity of zero.

If there are statistical dependencies among interspike intervals (i.e., the spike train is not a renewal process), this could only reduce the entropy further. For example, if the probability of observing a given interspike interval depends on the length of the previous interval, the true entropy would be lower than  $H_{\text{capacity}}$ . We did not generally have sufficient data to measure statistical dependencies between intervals. Therefore we use  $H_{\text{capacity}}$  as an upper bound on the true entropy rate of the binned spike train. In general the entropy of a spike train also depends on the time bin size, a relationship not explored here. We used the same bin size throughout (4.96 ms) for both  $H_{\text{capacity}}$  and estimating transmitted information.

**ESTIMATION OF TRANSMITTED INFORMATION.** The information transmitted by an LGN response about the stimulus contrast,  $H_{\text{trans}}$ , was estimated by computing the optimal linear reconstruction of the stimulus from the spike train (reviewed in detail in Rieke et al. 1997). Thus our perspective is to ask how well a hypothetical recipient of the neural response would be able to infer the stimulus. The stimulus property we reconstructed was its contrast, but we note that reconstructing any linear transform of the contrast by this method would have produced identical results. For example, the temporal derivative of the contrast is linearly related to the contrast; in our stimulus, the luminance at the receptive field center is also linearly related to contrast.

Figure 2 illustrates graphically this method of reconstruction and information estimation, using an example spike train from our data. Briefly, the spike train is convolved with a linear filter to obtain a reconstruction (Fig. 2A). The filter is chosen to be “optimal” in the sense of minimizing the mean squared error between this reconstruction and the original stimulus (see OPTIMAL LINEAR FILTER). The reconstruction is subtracted from the stimulus to obtain the “noise.” Figure 2B shows the power spectral densities of the stimulus and of the noise,  $P(s)$  and  $P(n)$ , respectively. Our stimulus update rate was 4.96 ms, or 201.6 frames per second. Thus we measure the power spectrum up to 100.8 Hz (the maximum frequency available for reconstruction is given by the Nyquist limit = sampling rate/2). The frequency range from 0 to 100.8 Hz was divided into 128 intervals, resulting in  $\Delta f = 0.79$  Hz.

The signal-to-noise ratio (SNR) as a function of temporal frequency is defined as  $\text{SNR} = P(s)/P(n) - 1$  (Fig. 2C). For random, Gaussian stimuli, the information transmitted by the spike train about a temporal frequency  $f$  in the stimulus has been shown to be at least  $\log_2 [1 + \text{SNR}(f)] \Delta f$  bits/s (Rieke et al. 1997). Thus an estimate of the total information transmitted by the spike train about the stimulus is given by

$$H_{\text{trans}} = \sum_{f=0}^{\text{CF}} \log_2 [1 + \text{SNR}(f)] \Delta f \text{ bits/s} \quad (3)$$

Observe that when  $\text{SNR} = 0$ , the information rate is  $\log_2 (1 + 0) = 0$  bits/s. We did not include frequencies above CF when computing  $H_{\text{trans}}$  because the power spectrum of the stimulus was essentially zero by construction, and errors would be caused by taking ratios of extremely small numbers.

**OPTIMAL LINEAR FILTER.** The optimal filter (Fig. 2D), expressed as a function of frequency, is uniquely given by  $h(f) = S_{AB}(f)/S_{AA}(f)$ , where  $S_{AB}(f)$  is the Fourier transform of the cross-correlation between the spike train (A) and the stimulus (B), and  $S_{AA}(f)$  is the Fourier transform of the autocorrelation of the spike train (Wiener 1949). If spikes were always farther apart than the extent of the filter

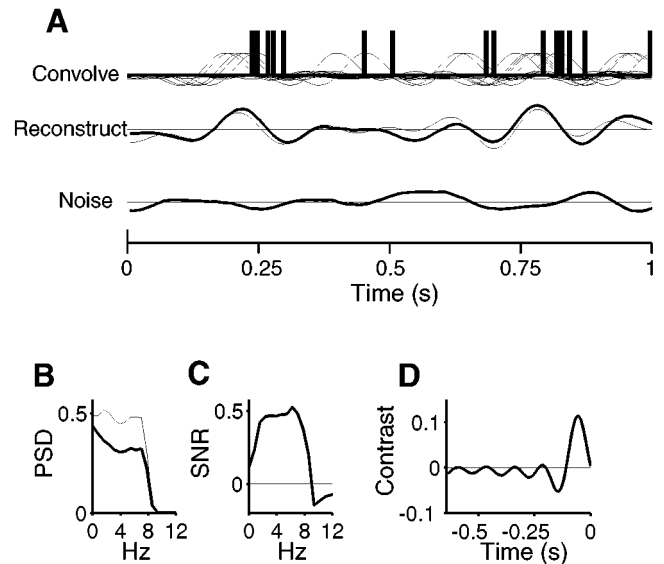


FIG. 2. Schematic of linear reconstruction method. *A: top plot* (“Convolve”) shows an example spike train, with a linear filter superimposed on the spike train at the time of each spike. This filter was chosen to be optimal in a sense explained in text. The *2nd plot* (“Reconstruct”) shows the sum of these superimposed filters (thick line), which is the reconstruction (the estimated deviation of the stimulus from the mean contrast). Superimposed (thin line) is the actual stimulus that elicited the spike train, expressed as  $C(t) - \mu$ , where  $C(t)$  is the grating contrast at time  $t$  and  $\mu$  is the mean contrast over the trial. The *3rd plot* (“Noise”) shows the reconstruction error, i.e., the difference between these 2 curves (stimulus – reconstruction), to be compared with the zero line. The *bottom two plots* show contrast on the same scale, with zero indicated by the horizontal line. *B.* The power spectral density (PSD) is plotted for the stimulus (thin line) and noise (thick line), in units of  $\text{Hz}^{-1}$ . Power spectra were computed by averaging the individual spectra of  $>100$  nonoverlapping short segments tapered by a Hanning window. *C:* the ratio of these spectra  $P(s)/P(n) - 1$  defines the signal-to-noise ratio (SNR), where  $\log_2 (1 + \text{SNR})$  is the transmitted information in bits (see text). *D:* the optimal linear filter plotted as a function of time, where  $t = 0$  is the time of an action potential. The horizontal line indicates zero.

in time, the optimal filter would be simply the average stimulus preceding a spike (sometimes called the “reverse correlation” or “spike-triggered average”). However, because spikes are often close enough together that filters overlap in time in the reconstruction, a correction is needed for the autocorrelation of the spike train. For a spike train completely unrelated to the stimulus, this filter is flat and equal to the mean of the stimulus.

For convenience of calculation, we computed an acausal filter, i.e., one that extends after as well as before the spike. This produced results numerically equivalent to those computed causally, as per Warland et al. (1997). Although the acausal filter is numerically defined at times after the spike, in practice spikes did not predict future stimuli (except to the extent that temporal correlations in the stimulus allowed the future stimulus to be predicted from the past stimulus). We computed filters that extended to 635 ms ( $128 \times 4.96$  ms time bins) before the spike. This filter length was chosen as the closest even power of two ( $2^7$ ) bins that amply exceeded the time needed for the filter amplitude to fall to zero for all cells.

To avoid overfitting of our data, we split the data from each trial in half, and used filters solved on each half to reconstruct the other half. Thus  $H_{\text{trans}}$  was calculated from reconstructions of stimuli not used to solve the filters. Therefore, it was possible to obtain negative values for  $H_{\text{trans}}$ , if the amount of data were inadequate such that the filters fit noise in the data.

This method provides strict lower bound on the transmitted information (Bialek et al. 1991; Rieke et al. 1997; Warland et al. 1997). In other words, this method entitles us to draw the strong conclusion that

the information content must be *at least* what we measured, because whenever we were forced to make assumptions in our analysis, we always chose assumptions that, if incorrect, could only cause us to underestimate information.

**ESTIMATION OF CODING EFFICIENCY.** The coding efficiency is the fraction of coding capacity used to transmit visual information. We estimate the efficiency by

$$E = H_{\text{trans}}/H_{\text{capacity}} \quad (4)$$

Because  $H_{\text{capacity}}$  is an upper bound (true entropy rate  $\leq H_{\text{capacity}}$ ), and  $H_{\text{trans}}$  is a lower bound (true transmitted information rate  $\geq H_{\text{trans}}$ ), it follows that  $E$  is a lower bound: the fraction of spike train variability used to encode visual information must be *at least*  $E$  (Rieke et al. 1993, 1997; Warland et al. 1997).

Burst responses have two properties that could affect the accuracy of this estimate. First, the reproducible ISI pattern within bursts implies that  $H_{\text{capacity}}$  is more of an overestimate of the entropy rate for bursts than for tonic spikes. We controlled for this possibility by also analyzing the bursts as unitary events (Bair et al. 1994). Second, bursts are highly nonlinear responses (Guido et al. 1995). Although some nonlinear encoding mechanisms are linearly decodable, it is possible that the visual information encoded by bursts is preferentially underestimated by the linear reconstruction method, compared with the information encoded by the more linear tonic responses. In both cases, if there is any error, it is likely to be in the direction of underestimating the coding efficiency of bursts relative to tonic responses. Thus our analysis is conservative with respect to the null hypothesis that bursts are not coding stimulus information.

## RESULTS

We recorded a total of 35 cells from 6 cats in response to random temporal visual stimuli. We concentrate below on the quantitative analysis of data from 25 cells from 4 cats, for which we used stimuli with the properties described in METHODS (Fig. 1). This population consisted of nine ON-center X cells, eight ON-center Y cells, four OFF-center X cells, and four OFF-center Y cells. The remaining data showed qualitatively similar trends, but could not be analyzed by the same quantitative methods because of differences in the stimulus design.

### *Bursts are distinctive firing events*

A representative short segment of the voltage trace from an LGN relay cell in response to the randomly fluctuating visual stimulus (Fig. 1) is shown in Fig. 3A. The events identified as bursts by our criteria are marked with stars. In all the cells we studied, we found that the responses contained bursts intermingled with tonic spikes, as has been described previously (Guido et al. 1992, 1995; Lu et al. 1992; Mukherjee and Kaplan 1995). We define the “burst fraction” as the fraction of action potentials in a trial that were found in bursts according to our ISI criterion (see METHODS). The X cells we recorded had a lower burst fraction ( $0.2 \pm 0.2$ , mean  $\pm$  SD) than the Y cells ( $0.6 \pm 0.3$ ).

Under our recording conditions, LGN cells did not exhibit sustained periods of burst (or tonic) mode, in the sense of extended stretches of time during which exclusively burst (or tonic) activity occurred. Nor was the occurrence of bursts oscillatory. We did not find any consistent relationship of the burst fraction with the stimulus parameters we varied. However, greater depth of anesthesia appeared to increase the burst fraction (data not shown) (see also Guido and Weyand 1995).

The distribution of successive pairs of ISIs could be ana-

lyzed in some very long trials, one of which is shown in Fig. 3B. For each action potential, a single point is plotted based on the preceding ISI (abscissa) versus the subsequent ISI (ordinate). The observed pattern is not that expected from a highly regular spike train, for which the points would fall on the diagonal. A conspicuous firing pattern observed in our data, evident as a clear cluster in this ISI plot, is the event identified by our burst criterion.

The shaded area at the *bottom right* of Fig. 3B defines the criterion for the first spike of a burst: a preceding interval of  $\geq 100$  ms, and a subsequent interval of  $\leq 4$  ms. All subsequent spikes in bursts must by definition lie within the shaded area on the *left* (preceding interval  $\leq 4$  ms). Those falling within the box at the *bottom left* are spikes within a burst (because the next interval is  $\leq 4$  ms, these are not the last spikes of bursts). The cluster near the closed arrow represents the final spikes in bursts that were followed by a short interval; the cluster near the open arrow represents the last spikes in bursts that were followed by a long interval. Some but not all of the latter spikes are followed by another burst. In this trial, 73% of the spikes were in bursts, with an average of 2.9 spikes per burst. In other words, about half of the independent firing events were bursts containing an average of about three spikes.

To further explore the degree to which bursts were stereotyped events, we measured the variability of the number of spikes in a burst within individual trials. Figure 3C shows, for the data shown in Fig. 3B, the distribution of the number of spikes in the bursts. All bursts by definition have at least two spikes, but the number of spikes per burst in this single trial varied from two to as many as five. This variability in burst size can be quantified by the coefficient of variation (CV), defined as the standard deviation divided by the mean. The CV of number of spikes in a burst in this trial was 0.26. This is less variability than would be found if the number of spikes had been determined by a Poisson process for a fixed duration, in which case the expected CV would be 1.0 (Gabbiani and Koch 1998; Papoulis 1984). Similar results were found for all cells in this study: the mean number of spikes per burst was  $3.0 \pm 1.4$  (X cells) or  $2.7 \pm 0.5$  (Y cells), and the CV of burst size within individual trials was  $0.25 \pm 0.11$  (X cells) or  $0.23 \pm 0.05$  (Y cells).

The timing of spikes within a burst was also stereotyped. The ISIs within a burst increased in length systematically. In the trial shown, the mean lengths for the first three intervals in a burst were 2.5, 3.0, and 3.4 ms, respectively; the mean length of the first postburst interval was much longer (360.3 ms; Fig. 3D). The sharp shoulder at 4 ms in the distribution of lengths for the later intervals in the bursts implies that some spikes that belong to a burst have not been classified as such due to the stringent 4-ms cutoff we impose on the ISI. The width of the distributions for within-burst intervals (SD is 0.4 for each of the 1st 3 intervals) indicates that the variability in the timing of spikes within burst was small. This variability was similar for all X and Y cells studied (not shown).

Taken together, the results presented in Fig. 3 confirm that in the responses to this novel dynamic stimulus, the burst criteria identify a frequent and stereotyped class of firing events having properties consistent with the bursts associated with the low-threshold calcium conductance.

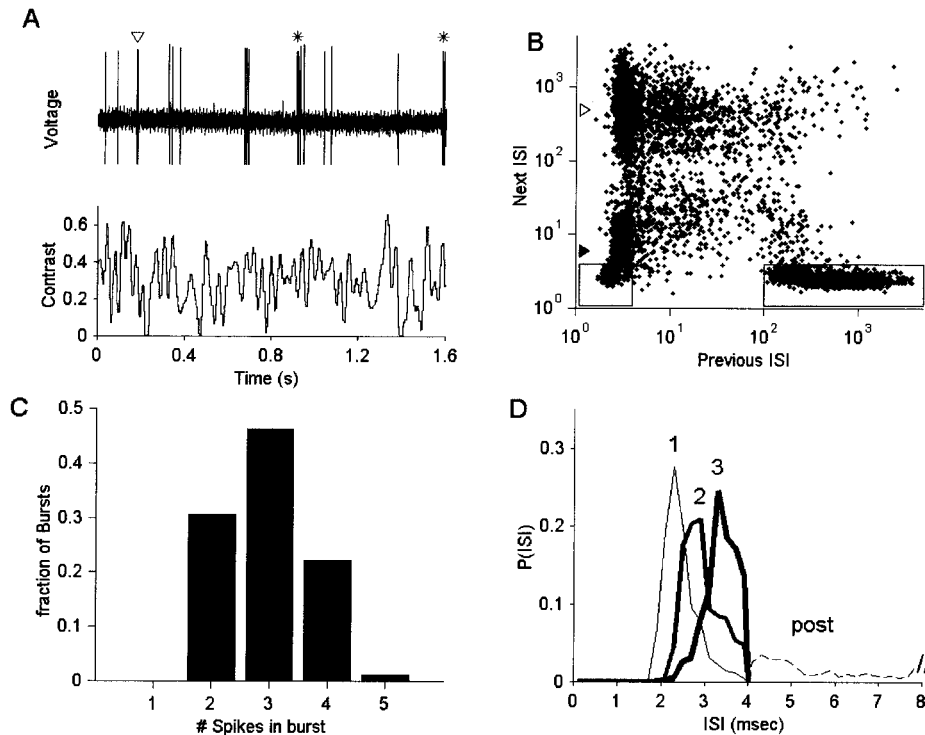


FIG. 3. Bursts are distinctive firing events. *A*: a short voltage trace from an ON-center Y cell is shown above the contrast of the visual stimulus. Both traces are shown at the 0.1-ms resolution of data acquisition. Stars (\*) mark the events that are classified as “bursts” by our interspike interval criterion. The cluster of spikes marked by the arrow is not considered a burst because of the absence of a 100-ms silence preceding the spikes. The low-amplitude high-frequency noise in these unfiltered voltage traces does not have a peak near 60 Hz. *B*: for each spike a point is plotted at the previous vs. subsequent interspike intervals, in units of ms, plotted on a log-log scale. Data are from 1 long (~20 min) trial from a representative ON-center Y cell with stimulus parameters  $\mu = 0.4$ ,  $\sigma = 0.2$ , CF = 8.0. Features indicated by shaded areas, boxes, and arrows are described in the text. *C*: probability distribution of the number of spikes in a burst, from the same data plotted in (*B*). By definition, all bursts have at least 2 spikes. *D*: probability distribution of interspike interval lengths for each interval within bursts. Data are from the same single trial as in *B* and *C*. The distribution for the 1st interval within bursts (thin black line, “1”) is based on all bursts containing  $\geq 2$  spikes ( $n = 1,645$ ). The 2nd interval (medium weight line, “2”) is based on all bursts with  $\geq 3$  spikes ( $n = 1,143$ ). The 3rd interval (thick line, “3”) is based on all bursts with  $\geq 4$  spikes ( $n = 382$ ). Bursts with  $\geq 5$  spikes were rare ( $n = 18$ ), so subsequent intervals were not analyzed. Part of the distribution of postburst intervals (dashed line, “post”) is also shown; the remaining 69% of postburst intervals were  $\geq 8$  ms (off the scale). Probabilities sum to one within each distribution. The binwidth of all histograms is 0.2 ms. By definition, within-burst intervals are  $\leq 4$  ms and postburst intervals are  $> 4$  ms. The absence of intervals  $< 1.6$  ms is due to the cell’s refractory period.

#### Within-trial comparison of bursts to tonic spikes

We show the response of an LGN relay cell at the *top* of Fig. 4A. The cell was responsive to the stimulus, in that its firing rate varied with time as more and less excitatory stimulus sequences occurred in the random pattern. For example, with the use of a sliding 100-ms window to compute a time-varying firing rate, the LGN response in this trial was  $< 10$  Hz 85% of the time, but exceeded 40 Hz 2% of the time, and reached 90 Hz at its peak.

The first step of our analysis was to identify the bursts in the LGN response and represent the burst and tonic spikes as separate “spike trains” for analysis (also shown in Fig. 4A). The “Tonic” channel contained all spikes not identified as parts of bursts. We either used all the spikes in each burst (“Bursts”), or represented each burst by a single event (“Burst Events”), as described in METHODS. The difference is that Burst Events lacked information about the *number* of spikes in the event. Neither representation was sensitive to the differences between bursts in the *timing* of spikes, because these differences were small (Fig. 3D) compared with our time bins (4.96 ms). We use the term spike train generically to refer to any kind of event

train, including Tonic, Burst, or Burst Event response components.

#### Information transmission

The stimulus reconstruction we obtained from each component spike train (as described in METHODS<sup>1</sup>) is shown in Fig. 4A. Based on these reconstructions, we estimated the amount of visual information each spike train contained, at each temporal frequency present in the stimulus. The results for this trial are shown in Fig. 4C. The similarity in the shapes of these curves (*inset*) indicates that all the temporal frequencies present in this stimulus were encoded equally well by either tonic or burst responses. When stimuli contained higher frequencies, we

<sup>1</sup> Figures 2 and 4–6 are related to one another hierarchically. In Fig. 2 (METHODS) we used a *single spike train* to illustrate the method by which we measure the transmission of visual information. In Fig. 4 we present the detailed results of such an analysis, for all the spike trains obtained from a *single trial*. We then demonstrate how the spike trains and their coding properties vary across trials for a *single cell* when the stimulus amplitude is varied in Fig. 5. Finally, we show the distribution of the key results over the entire *population of cells* in our study (Fig. 6).

A

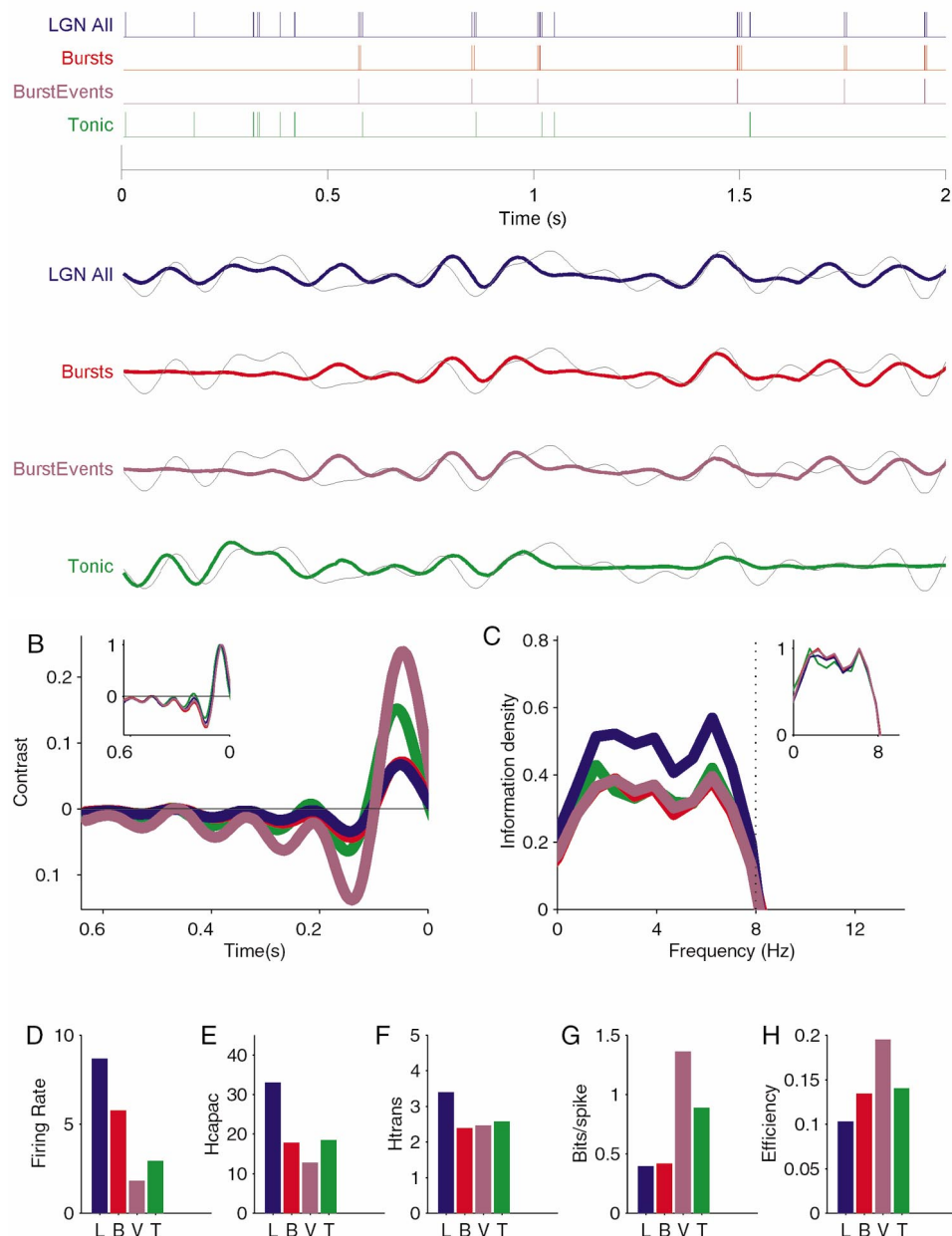


FIG. 4. Within-trial comparison of bursts to tonic spikes. *A*: response of a different ON-center Y cell to a stimulus with  $\mu = 0.4$ ,  $\sigma = 0.2$ , CF = 8.0 Hz. A short segment of a 20-min trial is shown. The spike trains analyzed are shown at *top*: the unprocessed spike train (“LGN All”) in blue, the spike train components (“Burst” in red and “Tonic” in green) after sorting by the interspike interval criteria, and the 1st spike of each identified burst (“Burst Events” in purple). For each spike train, the optimal linear reconstructions (thick lines) are compared with the original visual stimulus (thin black line) on the same time scale in the curves below. *A* serves as the color key for *B–H*. *B*: the optimal filter was solved separately for each spike train. The optimal filters as a function of time  $h(t)$  have amplitudes in units of stimulus contrast. *Inset*: same filters scaled to a peak of 1. *C*: visual information encoded by the reconstructions at each temporal frequency, expressed as the information density:  $\log_2 [1 + \text{SNR}(f)]$ , in units of  $\text{Bits s}^{-1} \text{Hz}^{-1}$ . The total information transmitted ( $H_{\text{trans}}$ ) is equal to the area under this curve in the interval  $0 < f < \text{CF}$ . *Inset*: same curves scaled to their respective peaks. *D*: time averaged firing rate of spike trains in units of spikes per second or Hz, where “spike” refers to an action potential for LGN (L), Bursts (B), and Tonic spikes (T), or an inferred  $I_t$  calcium spike for Burst Events (V). Average is over the entire trial. *E*: time averaged entropy rate or coding capacity ( $H_{\text{capacity}}$ ) of the spike trains in bits per second, based on the interspike interval distribution (not shown). *F*: average rate of transmission of visual information ( $H_{\text{trans}}$ ) by the reconstructions in bits per second. These values reflect the area under the curves in *C*. *G*: average amount of visual information encoded per spike (bits per spike), the ratio of values in *F* to those in *D*. *H*: average coding efficiency (*E*), the ratio of values shown in *F* to those in *E*.

sometimes observed qualitative differences in the shapes of these curves. However, longer recordings would have been necessary to determine the rolloff frequency from these high CF stimuli, because the estimation of the SNR at each frequency is noisier for broader band stimuli.

The overall transmission of visual information by each spike train ( $H_{\text{trans}}$ , Fig. 4*F*) is given by the area under each curve in Fig. 4*C*. The LGN response as a whole transmitted 3.4 bits/s of visual information about this stimulus. The tonic response transmitted 2.6 bits/s, and the bursts transmitted 2.4 bits/s, or 2.5 bits/s when they were treated as unitary events. To take into account differences in the number of events of each type (Fig. 4*D*), we expressed the information rate in units of bits per spike or event (Fig. 4*G*). We found that in this trial, the tonic spikes

carried more information per action potential (0.9 bits/spike) than the bursts (0.4 bits/spike), but bursts regarded as unitary events encoded more information per event (1.4 bits/event).

The coding capacity of a spike train depends on both the number of spikes and the regularity of the spike train. We estimated the information coding capacity of each of the spike trains of Fig. 4*A*, based on the entropy of their ISI histograms (not shown). This estimate,  $H_{\text{capacity}}$  (Fig. 4*E*), is the maximum information coding capacity for a spike train (binned at this resolution) that is consistent with the statistical regularity we observed (see METHODS). Although the burst response had many more spikes than the tonic response in this trial (Fig. 4*D*), the tonic spikes were more variable, such that both channels had about the same coding capacity (Fig. 4*E*).

The coding efficiency is defined as the fraction of the coding capacity used to carry information about this stimulus. On the basis of the maximum capacity (set by  $H_{\text{capacity}}$ ) and the minimum visual information (set by  $H_{\text{trans}}$ ), we could determine the minimum efficiency,  $E$  (Fig. 4H). In this trial, tonic spikes and spikes in bursts had about the same coding efficiency (14 and 13%, respectively), whereas bursts regarded as events were somewhat more efficient (19%).

#### Interpreting the optimal filters

To obtain the linear reconstructions discussed above, we computed the optimal linear filter for each spike type, based on the data from this trial (see ESTIMATION OF TRANSMITTED INFORMATION IN METHODS). These optimal filters are shown in Fig. 4B. The filters for tonic and burst responses have similar shapes, as revealed by scaling them all to the same peak (*inset*). The small amplitude oscillations in the filter reflect the temporal correlations in the visual stimulus, and depend on the temporal cutoff frequency CF (not shown). The large positive lobe between zero and  $-100$  ms reflects that this ON-center Y cell fired preferentially when the stimulus in the previous 100 ms was brighter than average in the receptive field center (and thus, darker than average in the immediate surround). The negative lobe between  $-100$  and  $-200$  ms indicates that the cell was also more likely to fire if this interval was preceded by a stimulus that was dark in the receptive field center (and thus, bright in the surround). In other words, the cell integrated over  $\sim 200$  ms, and responded best to *increases* in luminance in the center or *decreases* in luminance in the surround.

The similarity of the filter shapes can be measured by the correlation coefficient between them, which can range from zero (no correlation) to  $+1$  (perfect correlation) or  $-1$  (perfect anticorrelation). This measure is insensitive to linear scaling of the filters. In the example of Fig. 4B, the burst and tonic filters have a correlation coefficient of 0.92. We measured the correlation coefficient between the burst and tonic filter, for every trial in which both burst and tonic responses had at least 50 spikes encoding at least 0.1 bits per spike. We found that burst and tonic filter shapes were always similar (correlation coefficient  $0.83 \pm 0.11$ ,  $n = 74$  trials). We conclude that the two types of response always encoded *qualitatively* similar messages about the visual stimulus.

The complete analysis shown in Fig. 4 was performed for every individual trial, to compare the coding properties of bursts to tonic spikes within trials. The key results we obtained from each trial were the information rates (expressed in bits per spike or per event), and the coding efficiencies (expressed as a fraction of coding capacity) of each response type.

#### Effect of $\sigma$ on spike trains and visual coding

We varied the stimulus effectiveness by varying  $\sigma$ , the standard deviation of the contrast modulation. Figure 5 shows results from a single cell as the amplitude of the contrast modulation was increased from 0.01 to 0.20 in different trials. This covers the range from stimuli that are well below response threshold to ones that are well above it.

As the contrast modulations were made stronger, firing rates increased on average over the entire trial (not shown). The increase in firing rate with  $\sigma$  was variable and relatively mod-

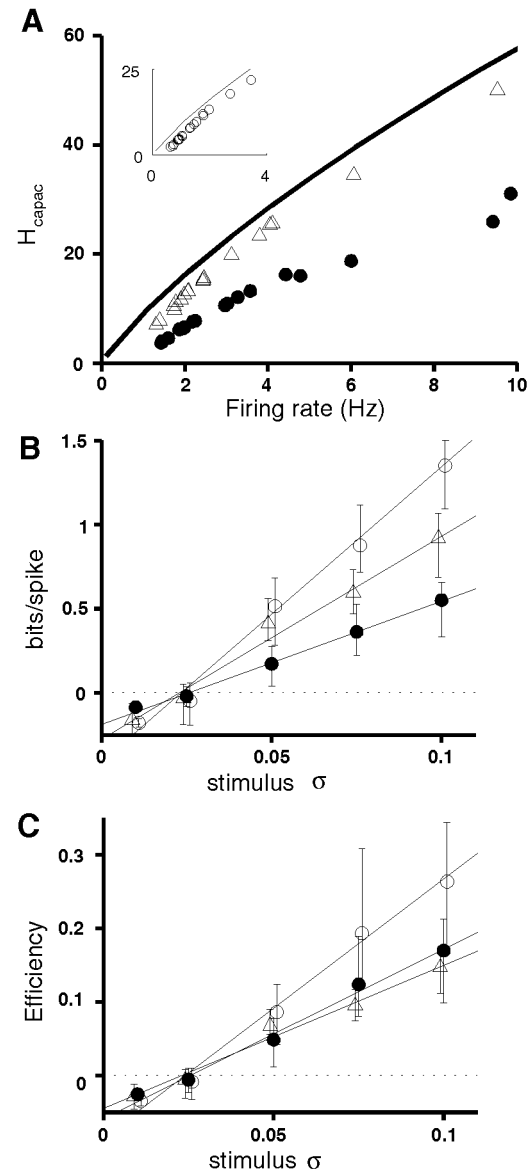


FIG. 5. Relative coding properties do not depend on absolute coding. *A*: relationship between firing rate and the coding capacity of the spike trains, for Bursts (closed circles), Tonic spikes (triangles), and Burst Events (open circles, *inset*). The stimulus parameter  $\sigma$  was varied from 0.01 to 0.2 across trials, holding constant  $CF = 16$  and  $\mu = 0.3$ . Each symbol represents a result from a single trial. All trials shown were recorded from a single OFF-center Y cell. Firing rate is defined as action potentials per second for Tonic or Bursts, or as bursts per second for Burst Events.  $H_{\text{capacity}}$  is defined in Eq. 2. The maximum possible entropy given the time bin size,  $H_{\text{max}}$  (see Eq. 1), is shown as a function of firing rate (solid line). *B*: visual information transmitted ( $H_{\text{trans}}/\text{firing rate}$ ) in bits/spike. Data and symbols as in *A*. At each value of  $\sigma$ , the mean result is shown by the symbol, with the range of values indicated by the bars. The  $\sigma$  values used were as follows: 0.01 ( $n = 2$  trials), 0.025 ( $n = 4$ ), 0.05 ( $n = 4$ ), 0.075 ( $n = 4$ ), and 0.10 ( $n = 4$ ). The symbols are plotted slightly offset for visibility. Least-squared fits are shown as lines. *C*: coding efficiency ( $E = H_{\text{trans}}/H_{\text{capacity}}$ ) as a function of  $\sigma$ , data and symbols as in *A*.

est, possibly due to adaptation to the amplitude of fluctuations in spatial contrast (Smirnakis et al. 1997b).

The spike train coding capacity ( $H_{\text{capacity}}$ ) increased with firing rate, but according to a different relationship for bursts and tonic spikes, as shown in Fig. 5A. Over the range of firing

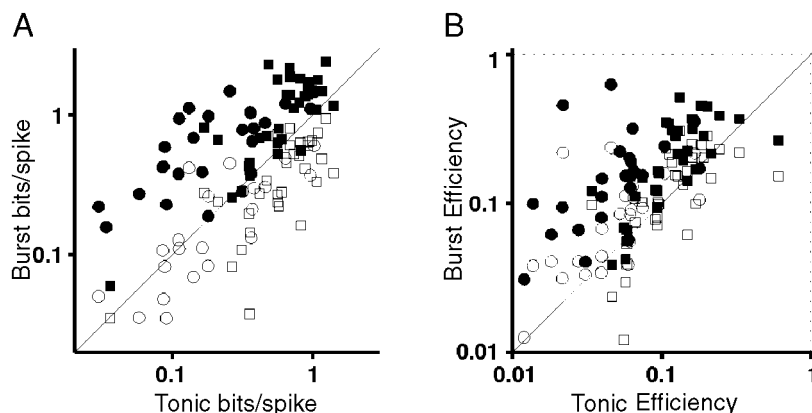


FIG. 6. Summary of within-trial comparisons of burst and tonic spikes. For this figure and for population statistics, we restricted analysis to trials in which  $\mu + 2\sigma \leq 0.77$ , to ensure that stimuli were well within the linear range of the contrast response of the monitor, and also excluded trials that did not have at least 150 events of each type to be analyzed. Each symbol represents a single trial of at least 4 min duration. Results are shown from 59 individual trials recorded from 15 cells. On average, results from 4 different stimuli are shown per cell. For statistics, we treat each cell as an independent observation, by determining the number of stimuli (trials) for which bursts were better than tonic spikes. We then used a binomial test of significance over cells. *A*: information rate, expressed in bits per spike ( $H_{\text{trans}}$  in bits/s divided by firing rate in spikes/s). Each open symbol compares the visual information transmitted by all the tonic action potentials (horizontal axis) to the information transmitted by all the action potentials in bursts (vertical axis) within a single trial. The closed symbols show the results for the same trials when bursts are treated as single events in the analysis. The information rate is then expressed in bits per event, where a single event is defined as either a tonic action potential or an entire burst. Circles are trials recorded from X cells, squares are trials recorded from Y cells. The diagonal corresponds to equality between the tonic and burst responses. *B*: coding efficiency ( $E$ ), the fraction of the spike train entropy that carries visual information. Data and key are as in *A*. Dashed lines indicate 100% coding efficiency.

rates observed, the coding capacity ( $H_{\text{capacity}}$ ) of the tonic spike trains was close to the maximum possible, given our chosen temporal resolution of 4.96 ms. The coding capacity of bursts was much lower than this maximum at any given firing rate. This reflects the greater regularity in burst firing patterns. When this regularity is taken into account, by treating bursts as unitary events, bursts then had close to maximal entropy. These results emphasize the importance of measuring the entropy of the spike trains, rather than using firing rate as an indirect measure of coding capacity.

The rate of transmission of visual information ( $H_{\text{trans}}$ ) increased with the amplitude of stimulus modulation. There was a baseline firing rate in the absence of stimulation, approximated by  $\sigma = 0.01$ , for which no visual information was encoded. Therefore, as  $\sigma$  and therefore  $H_{\text{trans}}$  increased, more information was encoded per spike (Fig. 5B), and the coding efficiency ( $E$ ) increased (Fig. 5C). In other words, the timing of spikes became increasingly determined by the stimulus.

We performed an equivalent analysis of each cell in our study. The amplitude of stimulus modulation determined the *absolute* coding properties of both burst and tonic responses, but we did not find any evidence that this affected their *relative* coding properties. Therefore we include trials from all stimuli in our population summary below.

### Population results

Whether measured in bits per event or in fractional coding efficiency, on a trial-by-trial basis the information encoded by the two response modes was similar. This is illustrated in Fig. 6 by the fact that all the points fall roughly along the diagonal. The approximate equivalence of burst and tonic spikes for coding this stimulus was supported by fact that ACPD reduced bursting (see METHODS), yet had little effect on visual coding. For 13 trials with a high burst fraction

( $0.45 \pm 0.14$ ), application of ACPD reduced the burst fraction by at least half (to  $0.03 \pm 0.03$ ) in the cell's response to a stimulus with the same parameters. Despite the change in burst fraction, there was no statistically significant change in the average firing rate, coding capacity, information rate, or coding efficiency (not shown).

Although burst and tonic modes were essentially similar, several small differences were statistically significant in the within-trial comparisons. In most trials, the amount of visual information encoded per burst was greater than per tonic spike (see closed symbols in Fig. 6A). Information per burst was on average 2.7 times greater than per tonic spike ( $P < 0.001$  by a binomial test, see legend). However, tonic spikes consistently encoded more information than bursts per action potential (1.8-fold more on average,  $P = 0.006$ , see open symbols in Fig. 6A). The coding efficiency ( $E$ ) was higher for bursts than for tonic spikes (Fig. 6B), regardless of whether all the spikes in the burst are considered (1.5-fold,  $P = 0.011$ ) or only the burst as an event (2.8-fold,  $P < 0.001$ ).

The Y cells in our population encoded more information about this visual stimulus than the X cells (i.e., circles, representing X cells, are below and to the left of squares, representing Y cells, in Fig. 6, A and B). However, the relative coding properties of bursts and tonic spikes were the same in both populations. The coding efficiency ( $E = H_{\text{trans}}/H_{\text{capacity}}$ ) of bursts was higher when bursts were treated as unitary events (closed symbols are above open symbols in Fig. 6B). We attribute this to two distinct reasons: the entropy rate ( $H_{\text{capacity}}$ ) was lower, and the visual information ( $H_{\text{trans}}$ ) was also higher (not shown). Thus the additional variability contained within bursts, considered at the temporal resolution of 4.96 ms, carried more noise than linearly decodable visual information (but see McCormick and Feeser 1990).

## DISCUSSION

*Bursts encode visual information*

We have shown that burst responses of LGN relay cells carry information about the time-varying contrast of randomly changing visual stimuli with temporal frequencies of up to 32 Hz. The coding efficiency of tonic and burst responses was roughly similar within individual trials, over a wide range of absolute coding efficiencies (Fig. 6). We found that both bursts and tonic spikes can have information rates exceeding 1 bit/spike. We observed examples of coding efficiency as high as 60% for tonic spikes and 63% for bursts treated as single events. In previous experiments using random stimuli and similar analysis methods, typical estimates of information rates in other sensory neurons were 1–3 bits per spike, and estimates of the average coding efficiency in other sensory neurons ranged from 11 to 60% (Bialek et al. 1991; Buracas et al. 1998; Rieke et al. 1993; 1995, 1997; Warland et al. 1997; Wessel et al. 1996).

These findings challenge the view that burst firing in the LGN is exclusively a feature of the sleeping or pathological brain (McCormick and Feuser 1990; Steriade 1992; Steriade and Llinás 1988; Steriade and McCarley 1990; Steriade et al. 1993). The fact that bursts participate in thalamic oscillations in normal sleep or in pathological conditions does not preclude the possibility that the same biophysical machinery could, in other circumstances, transmit useful data. Indeed, visually driven bursts have also been observed in the responses of LGN relay cells of awake, visually behaving cats (Guido and Weyand 1995) and monkeys (Ramcharan et al. 1998; P. Reinagel, unpublished analysis of data from McClurkin et al. 1991).

Our analysis was designed to be conservative with respect to assigning visual function to bursts. For this reason, we used a stringent criterion for identifying bursts. We also report only strict lower bounds on visual information content and coding efficiency, so that the information content and coding efficiency must be *at least* what we report. We estimated the information content of each response by an optimal first-order linear reconstruction. The result may be an underestimate, for three reasons: 1) additional information might be encoded in the spike trains in a form that could only be reconstructed using higher order (nonlinear) terms; 2) additional visual information might be encoded by spike time information at higher temporal resolution than the 4.96 ms time bins used; and 3) the use of the power spectra to estimate the information in the reconstruction entails a worst-case assumption that the errors are Gaussian. Moreover, our stimulus is unlikely to be optimal for the cell, and natural stimuli in particular may be much more efficiently encoded (Rieke et al. 1995). Therefore, future studies may well reveal additional visual information, and higher coding efficiencies, in both the burst and tonic responses of LGN relay cells.

*Bursts are efficient*

We did not find any evidence that bursts encode a special feature of the visual stimulus. However, we found that a relay cell in burst mode can transmit slightly more information in an event than the same cell in tonic mode (Fig. 6A), and does so with slightly less stimulus-unrelated response variability (Fig.

6B). These findings are consistent with prior indications that LGN bursts have selective advantages in the detection of periodic visual stimuli with comparable temporal frequencies (Guido et al. 1995).

There is precedent in other systems for the observation that bursts carry qualitatively the same information as isolated spikes, but with higher reliability (reviewed in Lisman 1997). In pyramidal cells of the electrosensory organ of the fish *Eigenmannia*, bursts and isolated spikes appear to detect similar stimulus features, but the burst response appeared to be a more reliable detector of the feature (Gabbiani et al. 1996). Similarly, ganglion cells of the salamander retina were found to fire discrete bursts (Smirnakis et al. 1996), and these bursts were preceded by a narrower distribution of possible stimuli than were single spikes (Smirnakis et al. 1997a).

*Temporal filtering by bursts*

Previous experiments *in vitro* showed that LGN bursts follow high-frequency stimulation poorly (McCormick and Feuser 1990), and *in vivo* experiments have suggested a role for bursts in filtering out high frequencies in visual stimuli (Mukherjee and Kaplan 1995). When we averaged SNR curves over trials and cells, we found that the average tonic SNR rolled off at somewhat higher frequencies than the average burst SNR, in both X and Y cell populations (not shown). From these population results, we cannot distinguish whether there is a direct causal connection between bursting and temporal filtering, or whether both filtering and bursting both result from some common cause, such as hyperpolarization. To explore this question further, it will be important to devise experiments that allow for within-trial comparisons, so that visual information in each frequency range may be attributed specifically to the burst events and tonic events within the responses of one cell under a single physiological condition.

*Control of burst mode*

We have shown that switching the response mode of the LGN cell has only minor consequences for the visual information content of the cell's response. Our experiments do not address what mechanisms normally determine the response mode during visual processing (but see Godwin et al. 1996b; Lu et al. 1993). Because burst mode reflects the activation of a voltage-dependent conductance, it could in principle be influenced by any of the cell's synaptic inputs, including cortical feedback (Sherman and Guillery 1996). Nonretinal inputs constitute the majority (90–95%) of the synapses onto LGN relay cells (Erisir et al. 1997), yet their function for vision is poorly understood. One possible function could be to modulate the response mode of an LGN cell, perhaps feeding back results of higher level visual processing or implementing an automatic bottom-up form of attention. Our data neither support nor exclude this possibility. If burst mode is controlled by such mechanisms, we conclude that the consequences for vision would probably not be found at the level of the information *encoded* by the LGN; the consequences of bursting might instead be found at the level of its *decoding*.

*Synaptic mechanisms*

The temporal pattern of action potentials could have important consequences for transmission of visual information across

the thalamocortical synapses (reviewed in Castro-Alamancos and Connors 1997b; Lisman 1997; see also Maass and Zador 1997). Based on our results, to maximize the recovery of visual information from the LGN, a synapse should transmit both bursts and single spikes reliably, and transmit bursts as unitary events. Indeed, layer 4 thalamocortical synapses with high transmission probability and paired-pulse depression (Castro-Alamancos and Connors 1996, 1997a; Stratford et al. 1996) might have these properties.

If other thalamocortical synapses are more like other cortical synapses, with low transmission probability and paired-pulse facilitation, these could transmit a distinct, burst-only information stream. For example, the layer 6 targets of LGN relay cells might have distinct information requirements. These cortical cells send axons back to the LGN to modulate relay cell responses (Godwin et al. 1996a,b; Sillito et al. 1994), and also project to the LGN cell targets in layer 4 to modulate the efficacy of the primary feed-forward projection (Ferster and Lindstrom 1985a,b; Katz 1987; Usrey and Fitzpatrick 1996; Wiser and Callaway 1996).

A direct test of these hypotheses will require measuring the postsynaptic potentials of cortical cells in response to a thalamic input spike train containing the pattern of ISIs of  $I_t$  bursts, as well as the ISI patterns characteristic of tonic LGN responses.

Computer programs used to generate stimulus sequences and for preliminary data analysis were generously shared by F. Gabbiani. We are indebted to B. Vaughan for adapting stimulus display software for the experiment.

P. Reinagel and C. Koch were supported by the Sloan Foundation Center for Theoretical Neuroscience as well as by the National Institute of Mental Health and National Science Foundation. D. Godwin and S. M. Sherman were supported by the National Institutes of Health.

Present address of D. Godwin: Dept. of Neurobiology and Anatomy, The Wake Forest University School of Medicine, Medical Center Blvd., Winston-Salem, NC 27157-1010.

Present address and address for reprint requests: P. Reinagel, Dept. of Neurobiology, Harvard Medical School, 220 Longwood Ave., Boston, MA 02115.

Received 25 August 1998; accepted in final form 15 December 1998.

## REFERENCES

- BAIR, W., KOCH, C., NEWSOME, W., AND BRITTEN, K. Power spectrum analysis of bursting cells in area MT in the behaving monkey. *J. Neurosci.* 14: 2870–2892, 1994.
- BAL, T. AND MCCORMICK, D. A. Synchronized oscillations in the inferior olive are controlled by the hyperpolarization-activated cation current  $I(h)$ . *J. Neurophysiol.* 77: 3145–3156, 1997.
- BIALEK, W., RIEKE, F., DE RUYTER VAN STEVENINCK, R. R., AND WARLAND, D. Reading a neural code. *Science* 252: 1854–1857, 1991.
- BURACAS, G. T., ZADOR, A. M., DEWEESE, M. R., AND ALBRIGHT, T. D. Efficient discrimination of temporal patterns by motion-sensitive neurons in primate visual cortex. *Neuron* 20: 959–969, 1998.
- CASTRO-ALAMANCOS, M. A. AND CONNORS, B. W. Spatiotemporal properties of short-term plasticity sensorimotor thalamocortical pathways of the rat. *J. Neurosci.* 16: 2767–2779, 1996.
- CASTRO-ALAMANCOS, M. A. AND CONNORS, B. W. Distinct forms of short term plasticity at excitatory synapses of neocortex and hippocampus. *Proc. Natl. Acad. Sci. USA* 94: 4161–4166, 1997a.
- CASTRO-ALAMANCOS, M. A. AND CONNORS, B. W. Thalamocortical synapses. *Prog. Neurobiol.* 51: 581–606, 1997b.
- COENEN, A. AND VENDRIK, A. Determination of the transfer ratio of cat's geniculate neurons through quasi-intracellular recordings and the relation with the level of alertness. *Exp. Brain Res.* 14: 227–242, 1972.
- COULTER, D. A., HUGUENARD, J. R., AND PRINCE, D. A. Calcium currents in rat thalamo-cortical relay neurons: kinetic properties of the transient low-threshold current. *J. Physiol. (Lond.)* 414: 587–604, 1989.
- CRICK, F. Function of the thalamic reticular complex: the searchlight hypothesis. *Proc. Natl. Acad. Sci. USA* 81: 4586–4590, 1984.
- ERISIR, A., VAN HORN, S. C., AND SHERMAN, S. M. Relative numbers of cortical and brainstem inputs to the lateral geniculate nucleus. *Proc. Natl. Acad. Sci. USA* 94: 1517–1520, 1997.
- FERSTER, D. AND LINDSTROM, S. Augmenting responses evoked in area 17 of the cat by intracortical axon collaterals of cortico-geniculate cells. *J. Physiol. (Lond.)* 367: 217–232, 1985a.
- FERSTER, D. AND LINDSTROM, S. Synaptic excitation of neurones in area 17 of the cat by intracortical axon collaterals of cortico-geniculate cells. *J. Physiol. (Lond.)* 367: 233–252, 1985b.
- FOURMENT, A., HIRSCH, J., MARC, M., AND GUIDET, C. Modulation of postsynaptic activities of thalamic lateral geniculate neurons by spontaneous changes in number of retinal inputs in chronic cats. 1. Input-output relations. *Neuroscience* 12: 453–464, 1984.
- GABBIANI, F. AND KOCH, C. Principles of spike train analysis. In: *Methods in Neuronal Modelling: From Ions to Networks*, edited by C. Koch and I. Segev. Cambridge, MA: MIT Press, 1998.
- GABBIANI, F., METZNER, W., WESSEL, R., AND KOCH, C. From stimulus encoding to feature extraction in weakly electric fish. *Nature* 384: 564–567, 1996.
- GODWIN, D. W. A tungsten-in-glass iontophoresis assembly for studying input-output relationships in central neurons. *J. Neurosci. Methods* 49: 211–223, 1993.
- GODWIN, D. W., VAN HORN, S. C., ERISIR, A., SESMA, M., ROMANO, C., AND SHERMAN, S. M. Ultrastructural localization suggests that retinal and cortical inputs access different metabotropic glutamate receptors in the lateral geniculate nucleus. *J. Neurosci.* 16: 8181–8192, 1996a.
- GODWIN, D. W., VAUGHAN, J. W., AND SHERMAN, S. M. Metabotropic glutamate receptors switch visual response mode of lateral geniculate nucleus cells from burst to tonic. *J. Neurophysiol.* 76: 1800–1816, 1996b.
- GUIDO, W. AND LU, S.-M. Cellular bases for the control of retinogeniculate signal transmission. *Int. J. Neurosci.* 80: 41–63, 1995.
- GUIDO, W., LU, S. M., AND SHERMAN, S. M. Relative contributions of burst and tonic responses to the receptive field properties of lateral geniculate neurons in the cat. *J. Neurophysiol.* 68: 2199–2211, 1992.
- GUIDO, W., LU, S. M., VAUGHAN, J. W., GODWIN, D. W., AND SHERMAN, S. M. Receiver operating characteristic (ROC) analysis of neurons in the cat's lateral geniculate nucleus during tonic and burst response mode. *Vis. Neurosci.* 12: 723–741, 1995.
- GUIDO, W. AND WEYAND, T. Burst responses in thalamic relay cells of the awake, behaving cat. *J. Neurophysiol.* 74: 1782–1786, 1995.
- JAHNSEN, H. AND LLINÁS, R. Electrophysiological properties of guinea-pig thalamic neurones: an in vitro study. *J. Physiol. (Lond.)* 349: 227–247, 1984a.
- JAHNSEN, H. AND LLINÁS, R. Ionic basis for the electroresponsiveness and oscillatory properties of guinea-pig thalamic neurones in vitro. *J. Physiol. (Lond.)* 349: 227–247, 1984b.
- KATZ, L. C. Local circuitry of identified projection neurons in cat visual cortex brain slices. *J. Neurosci.* 7: 1223–1249, 1987.
- LISMAN, J. E. Bursts as a unit of neural information: making unreliable synapses reliable. *Trends Neurosci.* 20: 38–43, 1997.
- LIVINGSTONE, M. S. AND HUBEL, D. H. Effects of sleep and arousal on the processing of visual information in the cat. *Nature* 291: 554–561, 1981.
- LU, S. M., GUIDO, W., AND SHERMAN, S. M. Effects of membrane voltage on receptive field properties of lateral geniculate neurons in the cat: contributions of the low-threshold  $Ca^{2+}$  conductance. *J. Neurophysiol.* 68: 2185–2198, 1992.
- LU, S. M., GUIDO, W., AND SHERMAN, S. M. The brain-stem parabrachial region controls mode of response to visual stimulation of neurons in the cat's lateral geniculate nucleus. *Vis. Neurosci.* 10: 631–642, 1993.
- MAASS, W. AND ZADOR, A. Computing with dynamic synapses. In: *Advances in Neural Information Processing Systems 10*. Cambridge: MIT Press, 1997.
- MACKEY, D. AND MCCULLOCH, W. S. The limiting information capacity of a neuronal link. *Bull. Math. Biophys.* 14: 127–135, 1952.
- MCCLEURKIN, J. W., GAWNE, T. J., RICHMOND, B. J., OPTICAN, L. M., AND ROBINSON, D. L. Lateral geniculate neurons in behaving primates. I. Responses to two-dimensional stimuli. *J. Neurophysiol.* 66: 777–793, 1991.
- MCCORMICK, D. A. Neurotransmitter actions in the thalamus and cerebral cortex and their role in neuromodulation of thalamocortical activity. *Prog. Neurobiol.* 39: 337–388, 1992.
- MCCORMICK, D. A. AND FEESER, H. R. Functional implications of burst firing and single spike activity in lateral geniculate relay neurons. *Neuroscience* 39: 103–113, 1990.

- MCCORMICK, D. A. AND VON KROSIGK, M. Corticothalamic activation modulates thalamic firing through glutamate "metabotropic" receptors. *Proc. Natl. Acad. Sci. USA* 89: 2774–2778, 1992.
- MUKHERJEE, P. AND KAPLAN, E. Dynamics of neurons in the cat lateral geniculate nucleus: in vivo electrophysiology and computational modeling. *J. Neurophysiol.* 74: 1222–1243, 1995.
- PAPOULIS, A. *Probability, Random Variables and Stochastic Processes* (2nd ed.). New York: McGraw-Hill, 1984.
- PETTIGREW, J. D., COOPER, M. L., AND BLASDEL, G. G. Improved use of tapetal reflection for eye-position monitoring. *Assoc. Res. Vis. Ophthalmol.* 18: 490–495, 1979.
- PRESS, W. H., TEUKOLSKY, S. A., VETTERLING, W. T., AND FLANNERY, B. P. *Numerical Recipes in C* (2nd ed.). Cambridge, UK: Cambridge Univ. Press, 1992.
- RAMCHARAN, E., GNADT, J., AND SHERMAN, S. State dependent changes in the firing pattern of relay neurons of the monkey LGN. *Soc. Neurosci. Abstr.* 24: 139, 1998.
- REINAGEL, P., GODWIN, D. W., KOCH, C., AND SHERMAN, S. M. Efficient information coding by LGN bursts. *Soc. Neurosci. Abstr.* 23: 171, 1997.
- RIEKE, F., BODNAR, D. A., AND BIALEK, W. Naturalistic stimuli increase the rate and efficiency of information transmission by primary auditory afferents. *Proc. R. Soc. Lond. B Biol. Sci.* 262: 259–265, 1995.
- RIEKE, F., WARLAND, D., AND BIALEK, W. Coding efficiency and information rates in sensory neurons. *Europhys. Lett.* 22: 151–156, 1993.
- RIEKE, F., WARLAND, D., DE RUYTER VAN STEVENINCK, R., AND BIALEK, W. *Spikes*. Cambridge, MA: MIT Press, 1997.
- SCHARFMAN, H. E., LU, S. M., GUIDO, W., ADAMS, P. R., AND SHERMAN, S. M. N-methyl-D-aspartate receptors contribute to excitatory postsynaptic potentials of cat lateral geniculate neurons recorded in thalamic slices. *Proc. Natl. Acad. Sci. USA* 87: 4548–4552, 1990.
- SHANNON, C. AND WEAVER, W. *The Mathematical Theory of Communication*. Urbana, IL: Univ. of Illinois Press, 1963.
- SHERMAN, S. M. AND GUILLERY, R. W. Functional organization of thalamocortical relays. *J. Neurophysiol.* 76: 1367–1395, 1996.
- SHERMAN, S. M. AND KOCH, C. The control of retinogeniculate transmission in the mammalian lateral geniculate nucleus. *Exp. Brain Res.* 63: 1–20, 1986.
- SILLITO, A. M., JONES, H. E., GERSTEIN, G. L., AND WEST, D. C. Feature-linked synchronization of thalamic relay cell firing induced by feedback from the visual cortex. *Nature* 369: 479–482, 1994.
- SINGER, W. Control of thalamic transmission by corticofugal and ascending reticular pathways in the visual system. *Physiol. Rev.* 57: 386–420, 1977.
- SMIRNAKIS, S., WARLAND, D., BERRY, M., AND MEISTER, M. Spike bursts in visual responses to retinal ganglion cells. *Soc. Neurosci. Abstr.* 22: 494, 1996.
- SMIRNAKIS, S., WU, E., AND MEISTER, M. The distribution of stimuli preceding a retinal ganglion cell burst. *Soc. Neurosci. Abstr.* 23: 1960, 1997a.
- SMIRNAKIS, S. M., BERRY, M. J., WARLAND, D. K., BIALEK, W., AND MEISTER, M. Adaptation of retinal processing to image contrast and spatial scale. *Nature* 386: 69–73, 1997b.
- STERIADE, M. Basic mechanisms of sleep generation. *Neurology* 42: 9–17, 1992.
- STERIADE, M. AND LLINÁS, R. R. The functional states of the thalamus and the associated neuronal interplay. *Physiol. Rev.* 68: 649–742, 1988.
- STERIADE, M. AND MCCARLEY, R. W. *Brainstem Control of Wakefulness and Sleep*. New York: Plenum, 1990.
- STERIADE, M., MCCORMICK, D. A., AND SEJNOWSKI, T. J. Thalamocortical oscillations in the sleeping and aroused brain. *Science* 262: 679–685, 1993.
- STRATFORD, K. J., TARCZY-HORNOCH, K., MARTIN, K.A.C., BANNISTER, N. J., AND JACK, J.J.B. Excitatory synaptic inputs to spiny stellate cells in cat visual cortex. *Nature* 382: 258–261, 1996.
- USREY, W. M. AND FITZPATRICK, D. Specificity in the axonal connections of layer VI neurons in tree shrew striate cortex: evidence for distinct granular and supragranular systems. *J. Neurosci.* 16: 1203–1218, 1996.
- VON KROSIGK, M., BAL, T., AND MCCORMICK, D. A. Cellular mechanisms of a synchronized oscillation in the thalamus. *Science* 261: 361–364, 1993.
- WARLAND, D. K., REINAGEL, P., AND MEISTER, M. Decoding visual information from a population of retinal ganglion cells. *J. Neurophysiol.* 78: 2336–2350, 1997.
- WESSEL, R., KOCH, C., AND GABBIANI, F. Coding of time-varying electric field amplitude modulations in a wave-type electric fish. *J. Neurophysiol.* 75: 2280–2293, 1996.
- WIENER, N. *Extrapolation, Interpolation and Smoothing of Stationary Time Series*. New York: Wiley, 1949.
- WISER, A. AND CALLAWAY, E. Contributions of individual layer 6 pyramidal neurons to local circuitry in macaque primary visual cortex. *J. Neurosci.* 16: 2724–2739, 1996.
- ZADOR, A. The impact of synaptic unreliability on the information transmitted by spiking neurons. *J. Neurophysiol.* 19: 1230–1238, 1998.